

Numerical stochastic analysis of groundwater contaminant transport and plume containment

Maged M. Hamed ^{a,*}, Philip B. Bedient ^b, Joel P. Conte ^c

^a *Department of Environmental Science and Engineering, and Center for Research on Parallel Computation, Rice University, 6100 Main Street, Houston, TX 77005-1892, USA*

^b *Department of Environmental Science and Engineering, Rice University, 6100 Main Street Houston, TX 77005-1892, USA*

^c *Department of Civil Engineering, Rice University, 6100 Main Street, Houston, TX 77005-1892, USA*

Received 6 October 1995; accepted 21 February 1996

Abstract

First- and second-order reliability methods (FORM and SORM) are applied as alternatives to the Monte Carlo simulation method in the probabilistic analysis of groundwater contaminant transport and remediation. A two-dimensional finite-element model is interfaced with a reliability analysis program to account for uncertainty in aquifer media. Hydraulic conductivity is modeled as a spatial random field with prescribed marginal probability distribution and correlation structure. FORM and SORM provide the probability that a contaminant exceeds a target level at a well, termed the probability of failure. Sensitivity of the probability of failure to basic uncertainty in grid block conductivities is also obtained, at no additional computational effort. Component reliability is used to analyze failure in a single well. Results indicate that, at the most likely failure scenario, grid block conductivities attain their maximum value near the source, the receptor well, and along the stream tubes connecting the two. System reliability is used to analyze the joint probability of failure at several wells in the aquifer. Results indicate that system failure probability is greater than the largest component failure probability. Correlation between component failure events is greater when the individual wells are closer. Sensitivity of the upper bound on system probability with respect to grid block conductivities is highest along the path the contaminant follows to reach the receptor wells. Furthermore, the probability of failure to contain a plume from escaping site boundaries is analyzed, along with the corresponding sensitivity information. Probability of failure to contain the plume decreases as the well pumping rate increases. The presence of regions of lower conductivity dramatically increases the probability of remediation failure. A careful analysis of aquifer material uncertainty and heterogeneity is vital to the success of groundwater remediation systems.

* Corresponding author.

Keywords: groundwater; plume containment; contaminant transport; remediation; probabilistic modeling; reliability analysis; system reliability; Monte Carlo simulation

1. Introduction

Porous media exhibit extensive intrinsic heterogeneity. Hydraulic conductivities that span orders of magnitude at the same site are not uncommon. Assessing the extent of contamination at a given site depends largely on the ability to accommodate this heterogeneity in the modelling process. This problem has led to a wealth of literature in the field of probabilistic, or stochastic, subsurface transport modeling in the past decade.

First- and second-order reliability methods (FORM and SORM) have been developed in the field of structural engineering in the past 20 years. These methods have been recently studied as an appealing alternative to other probabilistic tools for modeling groundwater problems. For example, reliability methods have been found to be much more computationally efficient than the Monte Carlo simulation method, especially for the case of low-probability events (Jang et al., 1994). Furthermore, reliability methods provide sensitivity measures at no extra computational effort. The ability of these analytical reliability methods to accommodate complete, as well as incomplete statistical information is also of great value for groundwater modeling.

In an earlier paper, we presented the application of FORM and SORM to simple analytical probabilistic groundwater models (Hamed et al., 1995). The developed models allowed for the assessment of the extent of groundwater contamination from a continuous leaking source at the screening level, accounting for aquifer-, chemical-, and source-related parameter uncertainty. Reliability methods were found to be very efficient in these types of analyses.

In this paper, we extend the application of these reliability methods to the numerical solution of the groundwater transport equation. The use of the resulting numerical model allows the consideration of the spatial random variability and correlation structure of the aquifer material. Furthermore, complex geometry and boundary conditions can be considered. The analysis of the probability of exceeding a target contaminant level at one or several wells is presented, using component and series system reliability, respectively. The effect of parameter uncertainty on the efficiency of plume containment strategies is also presented.

Jang et al. (1994) applied FORM and SORM methods to probabilistically model contaminant transport in one and two dimensions. They applied their code to estimate the probability of exceeding target concentrations at specific points, taking into account the spatial random variability of the input parameters, along with their spatial correlation. They concluded that the probability of failure increases as the correlation scale increases and approaches that obtained using the analytical transport model, which represents the transport in a perfectly correlated medium. The sensitivity analysis showed that the solution is most sensitive to hydraulic conductivity near both the source and target regions. They also found that the second-order reliability method, SORM, can handle large variance of the input parameters; something which is not possible with many of the current available techniques.

The work presented here extends their work in the sense that the formulation is similar, but more emphasis is given to issues like the analysis of failure at several wells in the aquifer, the use of reliability methods in plume containment and remediation, and the effect of the presence of a lower-conductivity lens on the estimated reliability.

2. First- and second-order reliability methods

Reliability methods have been extensively applied to problems of structural safety (Madsen et al., 1986; Melchers, 1987). Recently, the methods have been extended to groundwater problems (Sitar et al., 1987; Schanz and Salhotra, 1992; Wu and Cawfield, 1992; Cawfield and Wu, 1993; Gureghian et al., 1994; Jang et al., 1994; Hamed et al., 1995, 1996). In this section we present a brief review of reliability theory.

2.1. Component reliability analysis

Component reliability analysis is based on formulating a single scalar limit-state function, $g(\mathbf{X})$, that describes the performance of the problem, in which \mathbf{X} is an n -dimensional vector of random variables. When assessing the extent of groundwater contamination, the limit-state function tests whether the simulated contaminant concentration at a well exceeds some selected target value:

$$g(\mathbf{X}) = C_t - C(\mathbf{X}) \quad (1)$$

It is therefore clear that the n -dimensional space of random variables is subdivided into a “failure” domain and a “safe” domain, depending on whether the simulated concentration $C(\mathbf{X})$ exceeds the target, C_t . The boundary between failure and safe regions is expressed by the limit-state surface, $g(\mathbf{X}) = 0$.

The probability that the concentration at the well exceeds the predetermined target value is termed the “probability of failure”, and is given by:

$$P_F = P[g(\mathbf{X}) \leq 0] = P[C_t \leq C(\mathbf{X})] = \int_{g(\mathbf{X}) \leq 0} f_{\mathbf{X}}(\mathbf{x}) d\mathbf{x} \quad (2)$$

where $f_{\mathbf{X}}(\mathbf{x})$ denotes the joint probability density function of \mathbf{X} and the integration is performed over the failure domain. The estimation of the above n -fold integral is a formidable task. In fact, even classical numerical integration methods would fail to evaluate such an integral for large n . Simulation methods, such as the classic Monte Carlo simulation, have been used to estimate this probability integral. However, for large-number dimensional problems, and for small probability of failure, the Monte Carlo simulation method is computationally inefficient. In other words, the solution of the transport equations using the finite-element method will require a very large number of realizations of the random vector \mathbf{X} ; which can render the simulation approach practically infeasible. FORM and SORM provide a much more efficient way of approximating the above integral, especially for small probability of failure. Furthermore, the reliability methods provide sensitivity information at no additional computational burden, which the Monte Carlo simulation cannot provide. Note that the dimensionality increases when the problem scale increases, or when considering three-dimen-

sional problems, at which cases the number of random variables will considerably increase.

FORM and SORM are based on transforming the space of the physical random variables, \mathbf{X} , into the space of uncorrelated standard normal variables, \mathbf{U} , using a non-linear one-to-one mapping, $\mathbf{U} = \mathbf{T}(\mathbf{X})$. The transformation function \mathbf{T} depends on the types of statistical information available for the basic random variables, \mathbf{X} , and whether these random variables are statistically correlated (Der Kiureghian and Liu, 1986).

In this study, we assume that marginal probability distributions of individual variables, along with the correlation structure, in the form of a correlation function, are known. Therefore, the transformation into the standard normal space proceeds in two stages, following the Nataf model (Der Kiureghian and Liu, 1986). First, the basic random variables, \mathbf{X} , are transformed into a space of correlated standard normal variates, \mathbf{Z} , such that $Z_i = \Phi^{-1}[F_{X_i}(x_i)]$, where $\Phi[\]$ denotes the standard normal cumulative distribution function and $F_{X_i}(x_i)$ is the cumulative distribution function of X_i . The variates \mathbf{Z} have a correlation matrix \mathbf{R}_0 . The second step consists of transforming the vector \mathbf{Z} into the space of uncorrelated standard normal variates as follows:

$$\mathbf{U} = \mathbf{\Gamma}_0 \mathbf{Z} \quad (3)$$

where $\mathbf{\Gamma}_0$ is a lower triangular matrix resulting from the Cholesky decomposition of the correlation matrix of \mathbf{Z} , i.e. $\mathbf{\Gamma}_0 = \mathbf{L}_0^{-1}$ in which $\mathbf{R}_0 = \mathbf{L}_0 \mathbf{L}_0^T$. Elements of the matrix \mathbf{R}_0 are the correlation coefficients, $\rho_{z_i z_j}$. These, in turn, are related to the correlation coefficients, $\rho_{x_i x_j}$, of the basic random variables, \mathbf{X} , through the following implicit integral relationship (Der Kiureghian and Liu, 1986):

$$\rho_{x_i x_j} = \int_{-\infty}^{+\infty} \int_{-\infty}^{+\infty} \left[\frac{x_i - \mu_i}{\sigma_i} \right] \left[\frac{x_j - \mu_j}{\sigma_j} \right] \phi_2(z_i, z_j, \rho_{z_i z_j}) dz_i dz_j \quad (4)$$

where $\phi_2(z_i, z_j, \rho_{z_i z_j})$ is the bivariate normal density function of normal variates with zero means, unit variances, and correlation coefficient $\rho_{z_i z_j}$; μ_i and σ_i denote the mean and standard deviation of X_i , respectively. For each pair of marginal distributions, $F_{X_i}(x_i)$ and $F_{X_j}(x_j)$, and for a given correlation coefficient $\rho_{x_i x_j}$, the above equation can be iteratively solved to obtain $\rho_{z_i z_j}$. Liu and Der Kiureghian (1986a), however, provided a set of empirical formulae relating $\rho_{z_i z_j}$ to $\rho_{x_i x_j}$ for some known marginal distributions. This greatly simplifies the calculations and overcomes the tedious process of iterative solution.

FORM and SORM proceed to approximate the limit-state surface in the standard normal space at the point on the limit-state surface which is closest to the origin, called the "design point", \mathbf{u}^* . This point has the advantage of being the most likely failure point in the standard normal space, and therefore most of the probability volume in the failure domain is contributed by the region neighboring the design point. After the design point is obtained, the limit-state surface in the standard normal space is approximated using a hyperplane or hyper-paraboloid using FORM or SORM, respectively. The distance from the origin to the design point in the standard normal space is called the reliability index, β . This is a measure of the "reliability" of the component

against the “failure mode” under consideration, in the sense that it measures the distance to the failure domain. Larger β indicates lower P_F , and vice versa.

The determination of the design point is a crucial step in the reliability solution. This is accomplished by solving a constrained nonlinear optimization problem, in which the distance from the origin to a point on the limit-state surface is minimized. Algorithms typically used to solve this problem include the specialized HL–RF method (Hasofer and Lind, 1974; Rackwitz and Fiessler, 1978), the sequential quadratic programming (SQP) method, and the modified HL–RF method (Liu and Der Kiureghian, 1986b).

FORM replaces the limit-state surface by a tangent hyperplane at the design point in the standard normal space. FORM reliability index is given by the inner vector product:

$$\beta^{\text{FORM}} = \boldsymbol{\alpha}^* \cdot \mathbf{u}^* \quad (5)$$

where $\boldsymbol{\alpha}^*$ is the unit vector normal to the limit-state surface at the design point directed toward the failure region in the standard space. A first-order estimate of the probability of failure is then given by:

$$P_F \approx P_F^{\text{FORM}} = \Phi(-\beta^{\text{FORM}}) = 1 - \Phi(\beta^{\text{FORM}}) \quad (6)$$

The quality of the approximation provided by FORM depends on the extent of nonlinearity exhibited by the limit-state surface, especially in the neighborhood of the design point. If the limit-state function does not contain highly nonlinear terms, then the above first-order approximation of the probability of failure is sufficiently accurate for practical purposes. Otherwise, a second-order approximation provides a way to account for some of the nonlinearity of the limit-state surface at the design point. SORM approximates the limit-state surface using a second-order paraboloid fitted at the design point. Both curvature-fitted (Breitung, 1984) and point-fitted (Der Kiureghian et al., 1987) paraboloid approximations have been used successfully.

Through the process of solving a reliability problem, one obtains, at very little additional computational effort, sensitivity measures of the reliability results. The first set of sensitivities of the reliability index, β is with respect to variations in the coordinates of the design point in the standard normal space, and is given by:

$$\nabla_{\mathbf{u}^*} \beta^{\text{FORM}} = \boldsymbol{\alpha}^* = \frac{\mathbf{u}^*}{|\mathbf{u}^*|} \quad (7)$$

The $\boldsymbol{\alpha}^*$ vector, hence, gives a measure of the change in β^{FORM} when the coordinates of the design point \mathbf{u}^* are perturbed one at a time. In other words, this vector indicates the relative importance of the standard variates, u_i . The components of $\boldsymbol{\alpha}^*$ are often referred to as the sensitivity factors in structural reliability theory. Since $\boldsymbol{\alpha}^*$ is computed at the design point, the above sensitivity measure is obtained at no additional computational effort.

The sensitivity of β^{FORM} with respect to the coordinates of the design point in the physical space, which is more physically meaningful, are obtained by the chain rule of differentiation:

$$\nabla_{\mathbf{x}} \beta^{\text{FORM}} = (\nabla_{\mathbf{u}^*} \beta^{\text{FORM}}) \mathbf{J}_{\mathbf{u}^* \cdot \mathbf{x}} = \boldsymbol{\alpha}^* \mathbf{J}_{\mathbf{u}^* \cdot \mathbf{x}} \quad (8)$$

where

$$J_{u^*, x^*} = \left. \frac{\partial \mathbf{u}}{\partial \mathbf{x}} \right|_{u^*, x^*}$$

is the Jacobian of the transformation from the \mathbf{x} -space to the \mathbf{u} -space evaluated at the design point. Since the values of $\nabla_{\mathbf{x}} \cdot \beta^{\text{FORM}}$ are dependent on the units of \mathbf{x}^* , Der Kiureghian and Ke (1985) scaled this gradient vector by the diagonal matrix \mathbf{D} of the basic random variables, and normalized the resulting vector to yield the unit gamma sensitivity vector:

$$\gamma = \frac{(\nabla_{\mathbf{x}} \cdot \beta^{\text{FORM}}) \mathbf{D}}{|(\nabla_{\mathbf{x}} \cdot \beta^{\text{FORM}}) \mathbf{D}|} \quad (9)$$

Thus, the unit vector γ gives the sensitivities of β^{FORM} with respect to equally likely changes in the coordinates of \mathbf{x}^* , thus providing a measure of relative importance of the basic random variable X .

The sensitivity results provided by the first-order reliability method also may include the parametric sensitivity results; examples of which are the delta and eta sensitivity vectors defined by:

$$\delta_i = \left\{ \sigma_i \frac{\partial \beta}{\partial \mu_i} \right\}, \quad \eta_i = \left\{ \sigma_i \frac{\partial \beta}{\partial \sigma_i} \right\} \quad (10)$$

The delta vector gives the relative importance of the mean (central) values of the basic random variables, while the eta vector indicates the relative importance of the variabilities (measured in standard deviations) of the basic random variables. These sensitivity measures are obtained with only a minor computational effort.

2.2. System reliability analysis

In the preceding section, we have looked at cases where the state of the system is described by a single limit-state function, i.e. having a single ‘‘mode of failure’’. However, a situation can arise that necessitates the simultaneous consideration of several limit-state functions, for example, if we consider the probability that the contaminant concentrations at any of several points exceed a predetermined critical value. This is important in exposure assessment situations where the interest is on more than one point of human exposure in the aquifer, or when assessing the performance of a remediation scheme based on the likelihood of success to meet the target cleanup levels at every point in the aquifer. In this case, the state of the system is described by the states of its components:

$$g_i(\mathbf{X}) = C_i - C_i(\mathbf{X}) \quad (11)$$

where each limit-state function $g_i(\mathbf{X})$, $i = 1, \dots, m$, defines whether the target concentration C_i has been exceeded by the simulated concentration at point i ($i = 1, \dots, m$) in the solution domain.

By definition of the problem, *failure* of the system occurs if *at least* one of its component fails, that is, the system under consideration is a *series system*. Hence, the system failure probability can be expressed as:

$$P_F^{\text{system}} = P\left[\bigcup_{i=1}^m g_i(\mathbf{x}) \leq 0\right] = 1 - P\left[\bigcap_{i=1}^m g_i(\mathbf{x}) > 0\right] \quad (12)$$

The calculation of P_F^{system} is complicated due to the fact that the components $g_i(\mathbf{x})$ are usually statistically P_F dependent since they share some of the same basic random variables. Upper and lower bounds on the probability of failure of a series system can be obtained from the individual component failure probabilities, P_{F_i} , and the joint failure probabilities in any two modes, $P_{F_i F_j}$. The uni-modal bounds make use of the P_{F_i} terms only, and are given by (Madsen et al., 1986):

$$\max_{i=1}^m P_{F_i} \leq P_F^{\text{system}} \leq \sum_{i=1}^m P_{F_i} \quad (13)$$

The bi-modal Ditlevsen bounds (Ditlevsen, 1979) make use of the individual modal failure probabilities and the joint failure probabilities in any two modes:

$$P_{F_1} + \sum_{i=2}^m \max\left\{P_{F_i} - \sum_{j=1}^{i-1} P_{F_i F_j}, 0\right\} \leq P_F^{\text{system}} \leq P_{F_1} + \sum_{i=2}^m \left\{P_{F_i} - \max_{j < i} P_{F_i F_j}\right\} \quad (14)$$

The Ditlevsen bounds depend on the ordering of the failure modes (or components), F_1, F_2, \dots, F_m , and different orderings may correspond to the largest lower bound and the smallest upper bound. Practical experience suggests that the failure modes (i.e. g -functions) be numbered in a decreasing order of P_{F_i} (Madsen et al., 1986).

The modal and joint modal failure probabilities (P_{F_i} and $P_{F_i F_j}$, respectively) used in formulating the above uni- and bi-modal bounds were assumed to be exact failure probabilities. A first-order (FORM) approximation of these modal and joint modal failure probabilities are give by (Madsen et al., 1986):

$$P_{F_i} \approx P_{F_i}^{\text{FORM}} = \Phi(-\beta_i^{\text{FORM}})$$

$$P_{F_i F_j} \approx P_{F_i F_j}^{\text{FORM}} = \Phi(-\beta_i^{\text{FORM}})\Phi(-\beta_j^{\text{FORM}}) + \int_0^{\rho_{ij}} \phi_2(-\beta_i^{\text{FORM}}, -\beta_j^{\text{FORM}}, \rho) d\rho \quad (15)$$

In which ρ_{ij} denotes the correlation coefficient between the failure modes i and j linearized at their design point. This modal correlation coefficient is obtained as the inner product of the two unit normal vectors at the modal design points:

$$\rho_{ij} = \alpha_i^* \cdot \alpha_j^{*T} \quad (16)$$

The integral in Eq. (15) must be evaluated numerically. To avoid this numerical integration, Ditlevsen (1979) has proposed the following simple bounds on $P_{F_i F_j}^{\text{FORM}}$:

$$\max(p_1, p_2) \leq P_{F_i F_j}^{\text{FORM}} \leq p_1 + p_2 \quad \text{if } \rho_{ij} > 0$$

$$0 \leq P_{F_i F_j}^{\text{FORM}} \leq \min(p_1, p_2) \quad \text{if } \rho_{ij} < 0 \quad (17)$$

where

$$\begin{aligned}
 p_1 &= \Phi(-\beta_j^{\text{FORM}}) \Phi\left(-\frac{\beta_i^{\text{FORM}} - \beta_j^{\text{FORM}} \rho_{ij}}{\sqrt{1 - \rho_{ij}^2}}\right) \\
 p_2 &= \Phi(-\beta_i^{\text{FORM}}) \Phi\left(-\frac{\beta_j^{\text{FORM}} - \beta_i^{\text{FORM}} \rho_{ij}}{\sqrt{1 - \rho_{ij}^2}}\right)
 \end{aligned} \tag{18}$$

By substituting the above bounds on $P_{F_i F_j}^{\text{FORM}}$ in Eq. (14), the relaxed bi-modal bounds on P_F^{system} are obtained:

$$P_{F_1} + \sum_{i=2}^m \max\left\{P_{F_i} - \sum_{j=1}^{i-1} P_{F_i F_j, u}, 0\right\} \leq P_F^{\text{system}} \leq \sum_{i=1}^m P_{F_i} - \sum_{i=2}^m \max\{P_{F_i F_j, l}\} \tag{19}$$

in which $P_{F_i F_j, u}$ and $P_{F_i F_j, l}$ denote upper and lower bounds, respectively, on $P_{F_i F_j}$.

Finally, a measure of the "system" reliability can be presented by reporting the system reliability index, given by:

$$\beta^{\text{system}} = \Phi^{-1}(1 - P_F^{\text{system}}) \tag{20}$$

3. Applications

3.1. Probabilistic model formulation

The probabilistic model is obtained by interfacing a numerical groundwater finite-element model, FLOTTRAN, with a general-purpose reliability analysis program, CALREL (Liu et al., 1989). The finite-element code FLOTTRAN is developed by Dawson (1993), and is used here to solve the transport equation:

$$\frac{\partial}{\partial t} [\theta c_i + A(c_i)] - \nabla \cdot (\mathbf{D} \nabla c_i - \mathbf{u} c_i) = q \bar{c}_i + R_i(c_1, \dots, c_M) \tag{21}$$

in a three-dimensional spatial domain, $\Omega = [0, L_x] \times [0, L_y] \times [0, L_z]$. In the previous equation, c_i represents the concentration of species i ($i = 1, \dots, M$); θ denotes the water content; $A(c_i)$ models adsorption/desorption of species i ; \mathbf{D} is the hydrodynamic diffusion/dispersion tensor, which includes the effects of molecular diffusion and longitudinal and transverse dispersion; $\mathbf{u} = (u^x, u^y, u^z)$ is the Darcy velocity; R_i models chemical reactions between species (e.g., biodegradation); q represents flow rates at injection and production wells; and \bar{c}_i is the concentration at wells: \bar{c}_i is specified at injection wells, and $\bar{c}_i = c_i$ at production wells. Wells are treated as point sources and sinks in the code. For boundary conditions, the user can specify either Dirichlet or Neuman boundary conditions on each edge of the boundary of Ω . The user can also specify a constant or spatially varying initial condition.

The advection term in Eq. (21) is handled using an explicit (in time) higher-order Godunov procedure. This procedure is essentially a more accurate version of the

standard upwind differencing. The diffusion/dispersion terms are handled by centered finite differences in space and are implicit in time. Thus, a linear system of equations must be solved at each time step. This system is solved using preconditioned conjugate gradient iterations. Some of the appealing features of the code are the cell-by-cell and global mass conservation. Furthermore, strongly advective flow can be modeled with minimal oscillation and numerical diffusion. The underlying theory of the numerical solution scheme is explained in Dawson (1993).

The reliability analysis program CALREL was used in this work for two reasons; it has proven an efficient tool for solving reliability problems, and the fact that the code is reliable and robust.

The interface between the finite-element transport code and the reliability program is obtained through a FORTRAN 77 user defined subroutine. At each iteration in the process of determining the design point, this subroutine calls FLOTRAN to evaluate the limit-state function $g(x)$ and its gradient for a given realization of the discretized spatial random field x . The gradient which is required by the nonlinear optimization scheme is approximated using the central finite-difference method. Thus, the i th element of the gradient matrix is approximated by:

$$\frac{\partial g(X)}{\partial x_i} \approx \frac{g(x_i + \Delta x_i) - g(x_i - \Delta x_i)}{2\Delta x_i} \quad (22)$$

in which the step size Δx_i is chosen as a small fraction of the standard deviation of each random variable x_i . The combined FLOTRAN–CALREL code provides the probability of failure, reliability index, and sensitivity information.

3.2. Spatial random fields

In the following numerical probabilistic analyses, the hydraulic conductivity is modeled as a spatial random field, $w(s)$. It is assumed that the statistical information available on the aquifer property consists of pointwise (or marginal) probability distribution, $F_w(w)$, and the spatial correlation coefficient function, $\rho_{ww}(s_1, s_2)$ (i.e. second-order joint moments). Thus, it is a state of incomplete probability information which is made complete by assuming that the transformed random field, $V(s) = \Phi^{-1}[F_w\{w(s)\}]$, is Gaussian with zero mean, unit variance, and spatial correlation.

This probabilistic model is the random field version of the Nataf model defined earlier for multiple random variables. The spatial correlation structure of the hydraulic conductivity is considered to be of the exponential type. Thus,

$$\rho_{ww}(h) = \exp\left(\frac{-|h|}{\lambda}\right) \quad (23)$$

where $|h| = \|s_1, s_2\|$ is the lag (separation) distance; and λ denotes the correlation length. This formulation assumes statistical isotropy, i.e. the correlation coefficient function depends only on the distance between spatial locations and is independent of direction. The correlation length is a measure of the rate of random fluctuations of a random field. It corresponds to the distance over which the correlation coefficient drops from 1 to

0.368. The exponential function is used here since it has been shown to adequately describe the spatial correlation of the log-conductivity data (Bakr et al., 1978; Jang et al., 1994).

To perform a finite-element reliability analysis of a system, it is required to discretize the spatial random field considered. This means that the spatial random field will be represented by an equivalent set of random variables. The random field discretization method employed in this study is the midpoint discretization method. Here, the random field values are defined at a finite set of discrete points, which correspond to the midpoint (or centroid) of each finite element. Then the random field is represented in terms of a vector of random variables, X , the elements of which are correlated (Der Kiureghian and Ke, 1988). The correlation coefficient matrix is obtained directly from the correlation coefficient function $\rho_{ww}(h)$ and the separation distances between the centroids of the finite element.

4. Results

4.1. Component and system reliability analysis

In many groundwater contamination applications, we are interested in studying the reliability of more than one component in the solution domain. For example, we may be interested in the probability that the contaminant will exceed a predetermined level at any point along a property boundary. The compliance with the regulatory standards at more than one receptor well in the aquifer of interest is another example. In these situations, the problem is formulated in a *system reliability* framework, in which several limit-state functions are considered, one for every *component* of interest.

As an example, consider the case where a contaminant source leaks chemicals into an underlying groundwater aquifer. Assume that there exists a number of downgradient points of human exposure (i.e. wells). In this case, we have several limit-state functions, one at each well. The formulation is similar to Eq. (11).

In general, a system can be idealized as a series system, a parallel system, or a combination of the previous two. The problem of groundwater contamination is posed in a *series system* format since failure of *any* of the components constitutes failure of the system. In other words, in a multiple well compliance example, if the concentration at any of the wells exceeds the predetermined target value, the system has failed.

As an application example, consider the probability of exceeding 2.0 mg l^{-1} at any of the three observation wells given in Fig. 1. That is, the probability of failure to meet the 2.0 mg l^{-1} threshold after the 350-day simulation time is required. Table 1 lists the input data for this case study. In Table 2, the system reliability results are shown for first-order uni-modal, bi-modal, and relaxed bi-modal bounds. As expected for a series system, the system failure probability obtained is higher than the largest component failure probability ($P_{F_1}^{\text{FORM}} = 0.385$, $P_{F_2}^{\text{FORM}} = P_{F_3}^{\text{FORM}} = 0.224$). The bi-modal bounds are narrower than the relaxed bi-modal bounds, which are, in turn, tighter than the first-order uni-modal bounds.

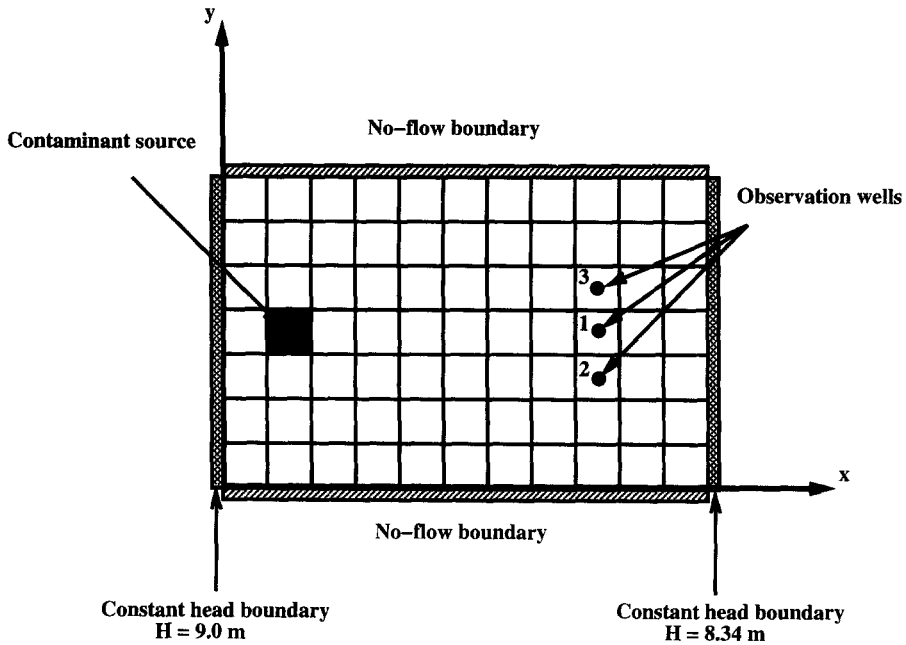


Fig. 1. Setup of the system reliability case study.

The correlation coefficient between the failure event at wells 1 and 2 is the same as that between wells 1 and 3 and equals 0.726. This means that failure to meet the target concentration of 2.0 mg l^{-1} at well 1 is closely related to the failure at well 2. A careful

Table 1
Input parameters for the system reliability case study

Deterministic data

Variable	Units	Value
Grid dimension, $\Delta x = \Delta y$	m	6.0
Aquifer thickness, H	m	6.0
Longitudinal dispersivity, α_x	m	0.2
Transverse dispersivity, α_y	m	0.02
Simulation time, t	day	350.0
Source concentration, C_0	mg l^{-1}	10.0
Target concentration, C_{target}	mg l^{-1}	2.0

Random field data

Variable	Units	Distribution/value
Hydraulic conductivity, K	cm s^{-1}	$\text{LN}(5.0 \times 10^{-3}, 5.0 \times 10^{-3})$
Correlation length, λ	m	18.0

LN(mean, standard deviation): lognormal.

Table 2
Results of the system reliability analysis for the 3-well case study

Method	Result	Value
First-order uni-modal bounds	bounds on P_F^{system}	$0.385 < P_F^{\text{system}} < 0.623$
	bounds on β^{system}	$0.291 > \beta^{\text{system}} > -0.331$
First-order relaxed bi-modal bounds	bounds on P_F^{system}	$0.385 < P_F^{\text{system}} < 0.543$
	bounds on β^{system}	$0.291 > \beta^{\text{system}} > -0.109$
First-order bi-modal bounds	bounds on P_F^{system}	$0.428 < P_F^{\text{system}} < 0.470$
	bounds on β^{system}	$0.182 > \beta^{\text{system}} > 0.075$

analysis of the physics of the problem explains this result. In order for the contaminant to exceed the target concentration at well 1, the grid block hydraulic conductivities at the design point should be high enough to allow easier and less resistive paths for the contaminant to reach the target well at the designated threshold value. The high-conductivity realizations also allow for more contaminant to reach well 2, hence resulting in a large correlation coefficient between the probability of exceeding the target level at wells 1 and 2. The correlation coefficient between the failure events at wells 2 and 3 is 0.217, which is less than the correlation between wells 1 and 2. This is explained by the fact that wells 2 and 3 are separated by a greater distance than wells 1 and 2, hence their failure events are correlated at a smaller value.

It should be noted that prior to the system reliability analysis, individual component reliability analyses are performed. The design point for well 1, which is the realization of hydraulic conductivity field corresponding to the most likely failure scenario at the observation well is shown in Fig. 2a. It is clear that the grid block hydraulic conductivities at the design point attain their maxima along the path lines connecting the source to the observation well. FLOTRAN is a block-centered solver. Therefore, the plot shows the midpoint conductivities, since the visualization program used can only interpolate between the midpoints inside the solution domain.

Gamma sensitivities for well 1 are displayed in Fig. 2b. As already mentioned, the gamma sensitivities provide a measure of the relative importance of equally likely changes in the basic random variables at the design point on the reliability estimate. Sensitivities are higher with respect to the hydraulic conductivity of the grid blocks along the path connecting the source to the observation well. Sensitivity information is very useful in designing future sampling at the site, in the sense that samples should be collected from spatial locations where the sensitivity of the probabilistic event is the highest. This will help reduce the uncertainty regarding the estimated probability of exceeding the predetermined concentration levels at the target observation well.

Fig. 2c shows the delta sensitivities for well 1. These provide the scaled variation of the reliability index due to an equally likely change in the mean value of the random variable. Negative sensitivities along the contaminant travel path indicate a decrease in the reliability index as the mean value of the hydraulic conductivity in this region increases. An increase in the hydraulic conductivity in the grid blocks that exhibit negative delta sensitivity will cause more contaminant to reach the target observation

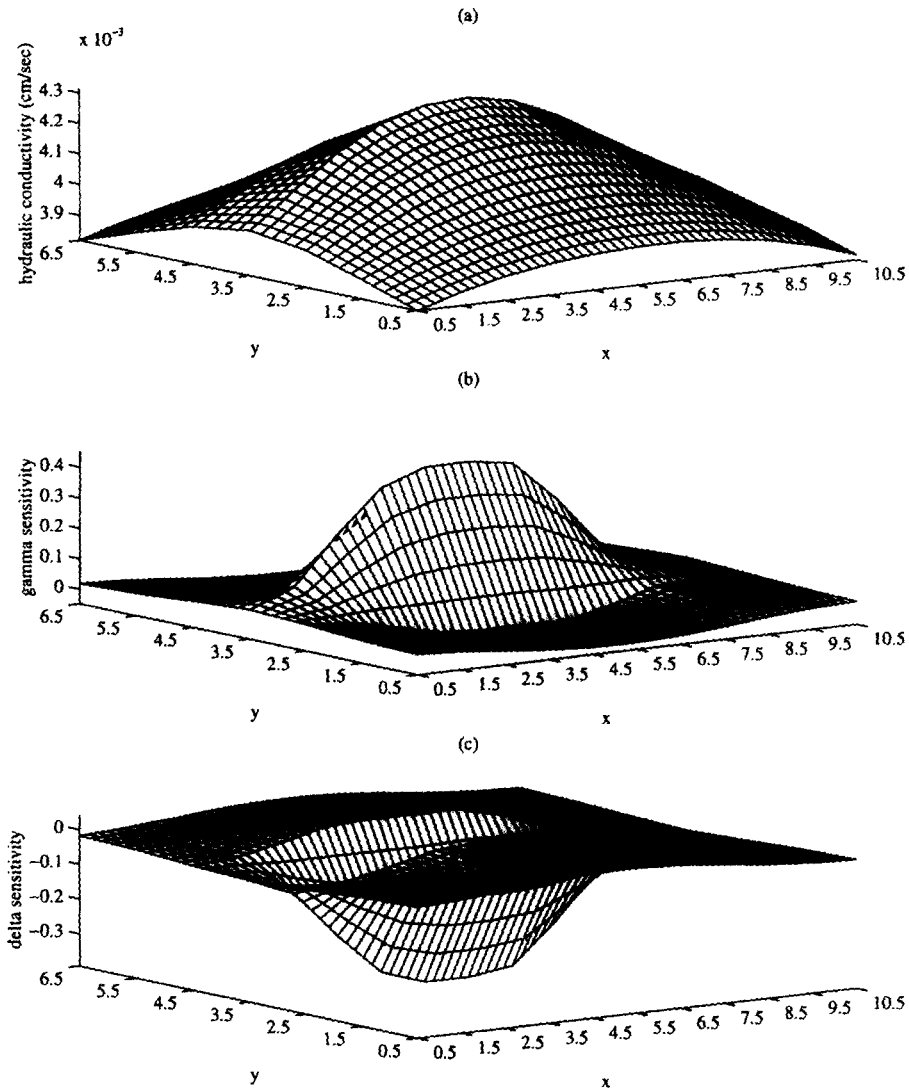


Fig. 2. Results for well 1: (a) design point; (b) gamma sensitivity; and (c) delta sensitivity.

well within the specified simulation time. Therefore, the probability of exceeding the target concentration level will increase, and the reliability index will decrease. The reverse is also true.

Fig. 3a-c illustrates the design point, gamma, and delta sensitivities for well 2. The same behavior is noticed for the design point and sensitivities as they exhibit their maximum values along the flow paths from the source to the target well.

Additional information gained from the system reliability analysis is the sensitivity of the system failure probability with respect to changes in the distribution parameters of

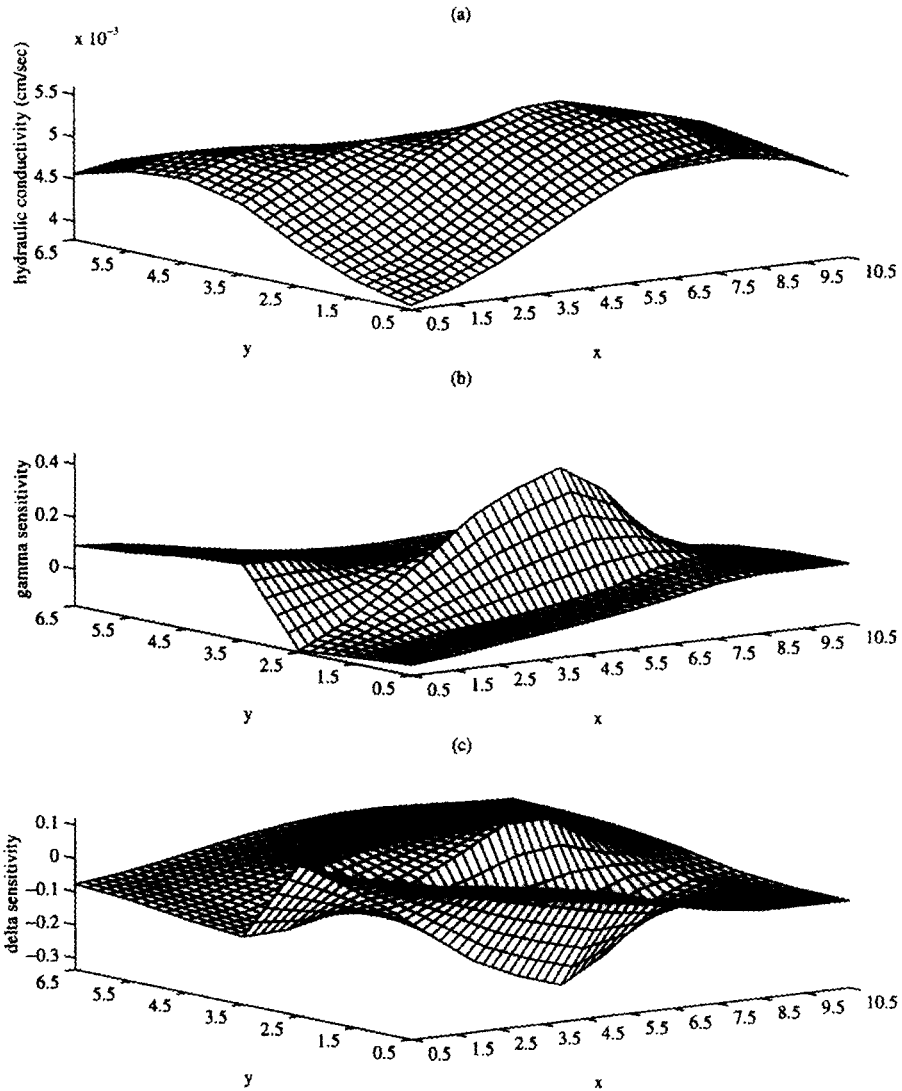


Fig. 3. Results for well 2: (a) design point; (b) gamma sensitivity; and (c) delta sensitivity.

the grid block conductivities. Fig. 4a displays the sensitivities of the upper bi-modal bound on P_F^{system} with respect to changes in the local mean value of the hydraulic conductivities. The results indicate that the greater the mean hydraulic conductivity of the region along the flow paths, the greater the system failure probability, a behavior easily explained by the earlier discussion.

Next, we look at the series system reliability in which only wells 2 and 3 are included. In this case, the system failure probability bounds are given in Table 3. The system failure probability in this case is less than in the case with three wells, as

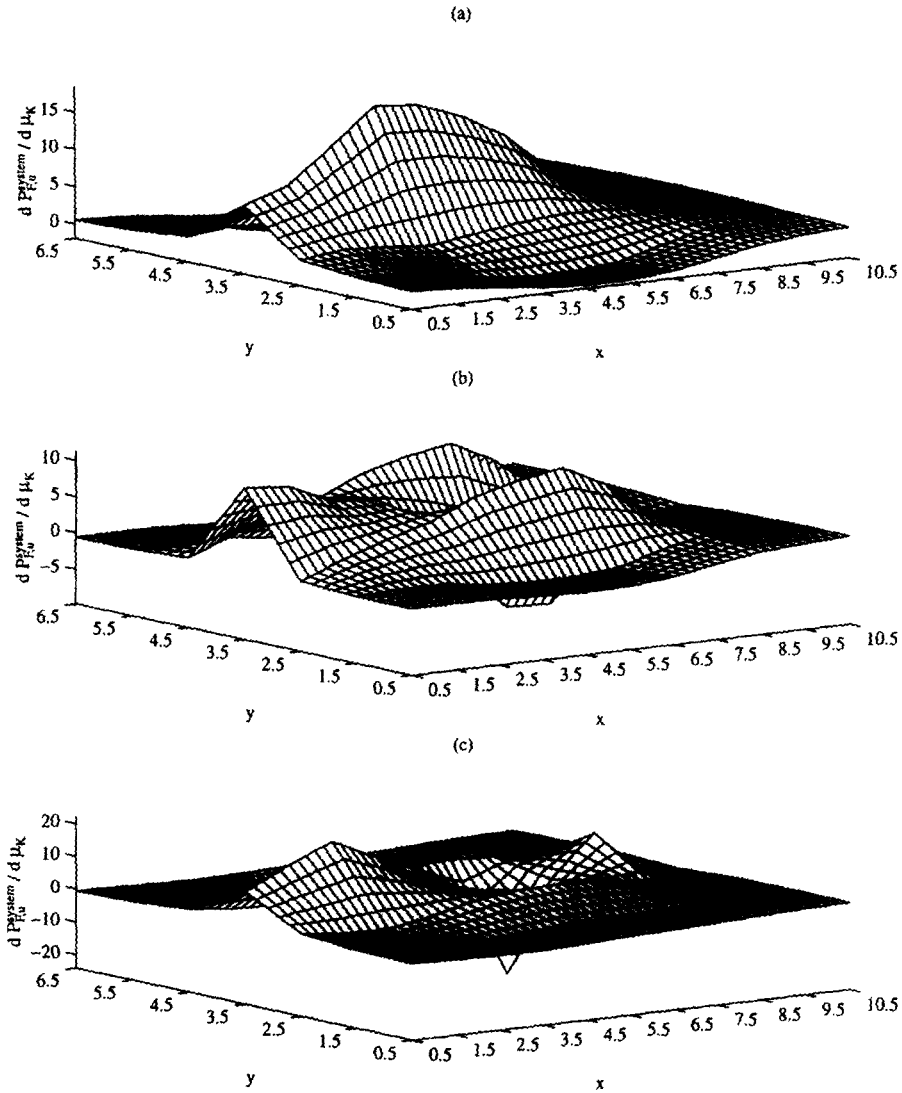


Fig. 4. Sensitivity of the upper bi-modal bound on the system failure probability to the local mean hydraulic conductivity: (a) for the 3-well case; (b) for the 2-well case; and (c) for 2-well with lower-conductivity lens.

expected. Fig. 4b depicts the sensitivities of the upper bi-modal bounds of system failure probability with respect to changing the mean value of grid block conductivities for the 2-well case. The pattern in which the sensitivities behave is interesting. Mean hydraulic conductivities along the branching path leading to both wells 2 and 3 have the highest impact on the system failure probability. The negative sign indicates an inverse relationship between local mean conductivity and system failure probability.

When a lower-conductivity lens is considered to exist between the two wells and in an orientation parallel to the mean groundwater flow direction (Fig. 5), the first-order

Table 3
Results of the system reliability analysis for the 2-well case study

Method	Result	Value
First-order uni-modal bounds	bounds on P_F^{system}	$0.224 < P_F^{\text{system}} < 0.398$
	bounds on β^{system}	$0.759 > \beta^{\text{system}} > 0.259$
First-order relaxed bi-modal bounds	bounds on P_F^{system}	$0.326 < P_F^{\text{system}} < 0.387$
	bounds on β^{system}	$0.450 > \beta^{\text{system}} > 0.287$
First-order bi-modal bounds	bounds on P_F^{system}	$0.377 < P_F^{\text{system}} < 0.377$
	bounds on β^{system}	$0.313 > \beta^{\text{system}} > 0.313$

bi-modal bounds on system failure probability changes from 0.377 to 0.369. In other words, the presence of the lower-conductivity lens affected the system reliability only very slightly. However, the sensitivity of the system failure probability with respect to the local mean hydraulic conductivity in this case differs considerably from the case without the lens. This is shown in Fig. 4c.

4.2. Remediation / containment under uncertainty

The impact of parameter uncertainty on achieving remediation/containment goals is important. Failure to account for such uncertainty can dramatically hinder the efficiency

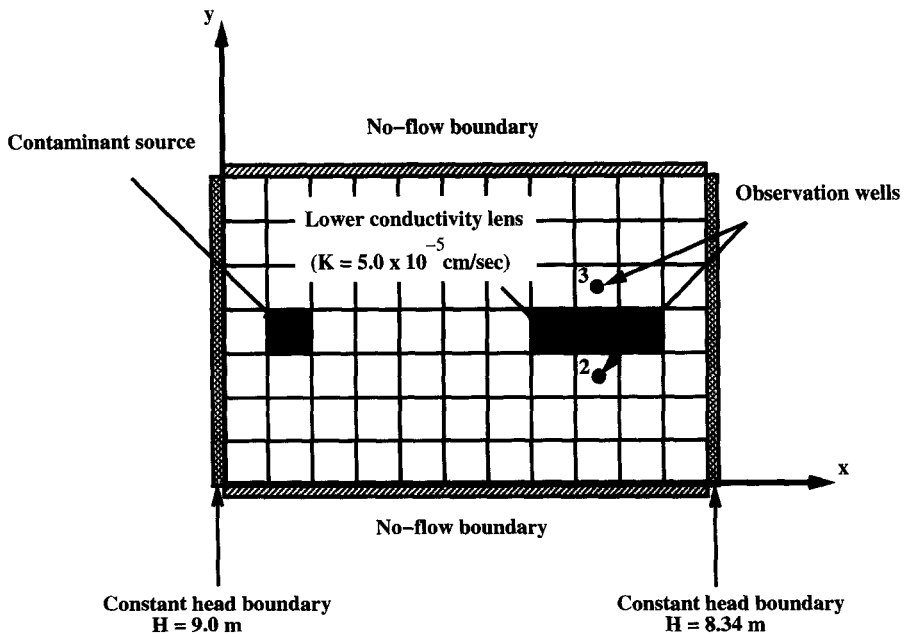


Fig. 5. Setup of the system reliability case with a lower-conductivity lens.

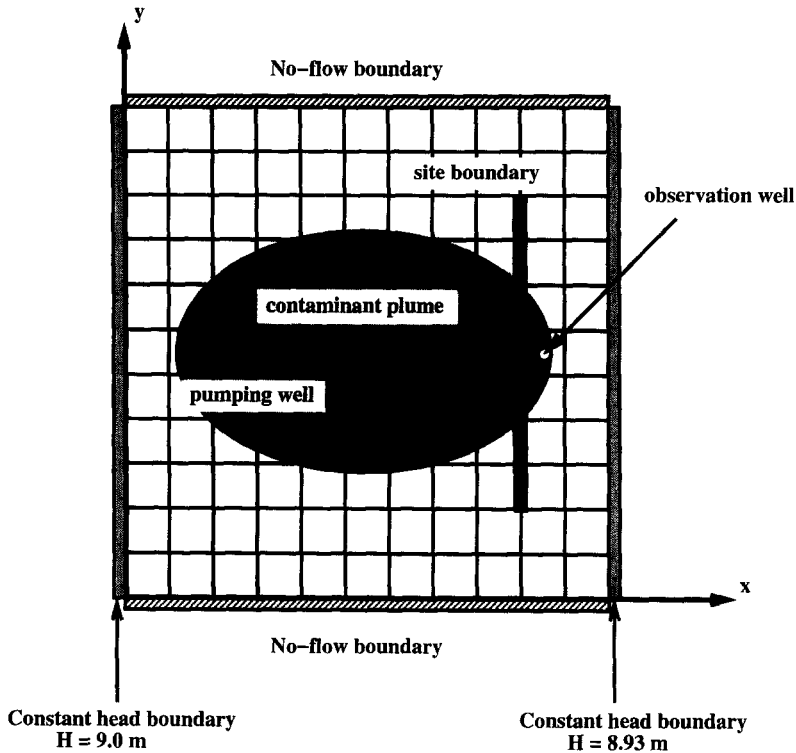


Fig. 6. Setup of the plume containment case study.

of the remediation/containment scheme, creating significant economic ramifications. In this section, we present a reliability formulation to study the effect of the natural variability of the hydraulic conductivity on achieving a plume containment goal. The limit-state function is formulated as in Eq. (1), however, C_i in this context is the remediation/containment threshold or target concentration at a specific well. *Failure* in this case indicates failure to contain the plume from reaching the observation well, or failure to remediate the plume to the predetermined threshold level.

Fig. 6 illustrates the problem setup. The aquifer's extent is 66.0 m on the side. A numerical grid of 11×11 is used to discretize the solution domain. The random field mesh used to discretize the spatial random field of hydraulic conductivity is assumed to coincide with the numerical mesh. That is, the number of random variables is $11 \times 11 = 121$, comprising the hydraulic conductivity in the center point of each grid block. Table 4 lists the input parameters for this case study. It should be noted that the hydraulic gradient is assumed constant throughout the case studies. The initial contaminant plume is shown in Fig. 7.

It is assumed that a property boundary is located as shown in Fig. 6. A pumping scheme is installed in such a manner so as to contain the plume from escaping into the neighboring property beyond the site boundary within the 30-day pumping period. The target concentration at the observation well is chosen, arbitrarily, to be 1.0 mg l^{-1} . In

Table 4
Input parameters for the plume containment case study

Deterministic data

Variable	Units	Value
Grid block dimension, $\Delta x = \Delta y$	m	6.0
Aquifer thickness, H	m	6.0
Aquifer porosity, θ	$\text{m}^3 \text{m}^{-3}$	0.35
Longitudinal dispersivity, α_x	m	3.0
Transverse dispersivity, α_y	m	0.3
Hydraulic gradient, i	m m^{-1}	0.001
Simulation time, t	day	30.0
Pumping rate, q	l s^{-1}	1.26

Random field data

Variable	Units	Distribution/value
Hydraulic conductivity, K	cm s^{-1}	$\text{LN}(2.0 \times 10^{-3}, 2.0 \times 10^{-3})$
Correlation length, λ	m	12.0

LN(mean, standard deviation): lognormal.

realistic applications, the target concentration and well location are chosen according to: (1) the type of contaminant; (2) land use at the neighboring property; and (3) risk estimation at the receptor well.

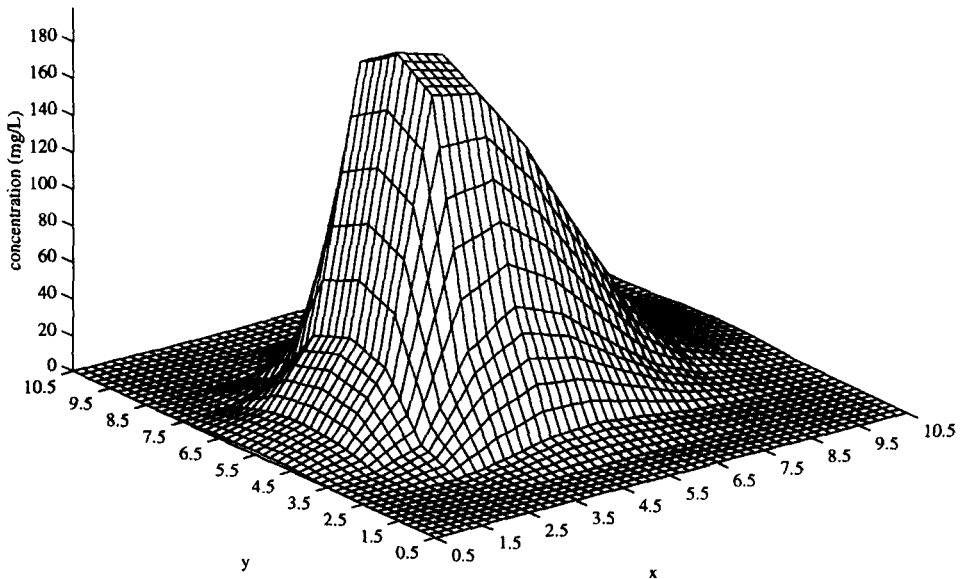


Fig. 7. Initial contaminant plume (mg l^{-1}).

Table 5

Failure probabilities for the remediation case study for pumping rate = 2.52 l s^{-1} (40.0 gpm)

Method	Failure probability	Reliability index
FORM	0.292	0.547
SORM ^a	0.343	0.405
SORM ^b	0.337	0.421
MCS	0.334	0.429

^a Improved breitung; ^b Tvedt's exact integral.

The numerical reliability model is used to estimate the probability of failure of the remediation/containment scheme. FORM failure probability and reliability index were found to be 0.743 and -0.655 , respectively. This means that if a single, fully penetrating well at the middle of the domain is pumped at a rate of 1.26 l s^{-1} (20 gpm) for 30 days, there will be a 74% probability of failure to contain the plume from reaching the downgradient observation well at a concentration exceeding the target concentration of 1.0 mg l^{-1} . The negative reliability index simply means that the probability of failure exceeds 0.5. This is clear by an examination of the definition of the relationship between P_F and β given in Eq. (6).

Next, the pumping rate is increased to 1.89 and 2.52 l s^{-1} (30.0 and 40.0 gpm), and the reliability analysis is repeated to study the effect of increasing the pumping rate on the failure probability. For the 1.89 l s^{-1} (30 gpm) case, FORM failure probability and reliability index are 0.41 and 0.227, respectively. Table 5 lists FORM, SORM, and Monte Carlo results for the 2.52 l s^{-1} (40.0 gpm) scenario. FORM and SORM results were in good agreement with that of the Monte Carlo simulation method. This good agreement in the reliability to that of the Monte Carlo results was observed for all of the case studies conducted. Thus, an increase in the pumping rate from 1.26 to 2.52 l s^{-1} (20.0 to 40.0 gpm) caused the failure probability at the observation well to drop from 74% to $\sim 33\%$. The design point, gamma and delta sensitivities for this case study are shown in Fig. 8a, b and c, respectively. It is interesting to see that the probabilistic event is most sensitive to hydraulic conductivities in the region downgradient from the pumping well. This is due to the fact that the more conductive this region is, the more "clean" water the pump is able to flush towards the observation well, and the better the containment becomes. This is indicated by the positive delta sensitivities in that region, which indicates a direct proportionality between the local mean value of the hydraulic conductivity in that region and the reliability index.

Next, we look at the impact of the presence of a lower-conductivity lens down-gradient from the pumping well, and upgradient from the observation well, as shown in Fig. 9. The lens has a conductivity of $2.0 \times 10^{-5} \text{ cm s}^{-1}$, which is two orders of magnitude less than the prevailing hydraulic conductivity. When the pumping rate of 1.89 l s^{-1} (30.0 gpm) was applied to this case, the probability of failure to meet the target concentration of 1.0 mg l^{-1} dramatically increased to 0.985, with a reliability index of -2.12 . This illustrates the significant impact that material heterogeneity and the presence of lenses have on the success of cleanup schemes. Table 6 lists FORM failure probability and reliability index for different pumping rates. For each pumping rate, the

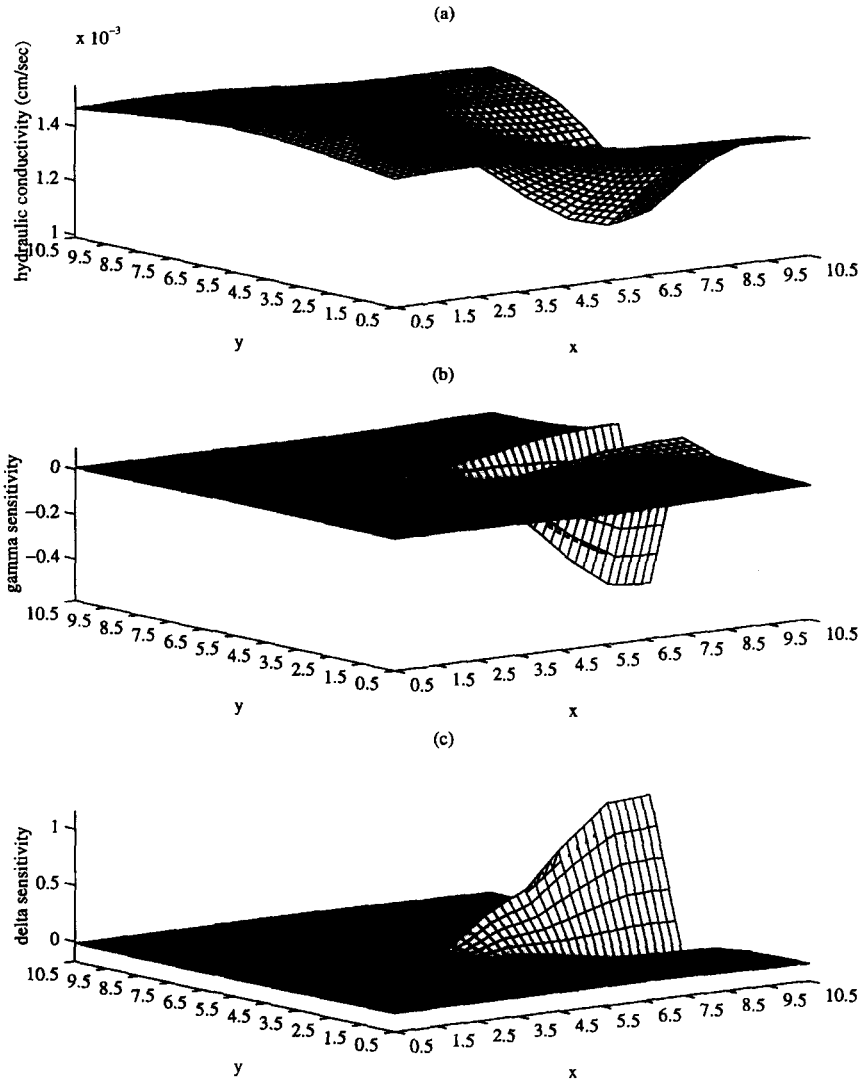


Fig. 8. Results for the plume containment case study (pumping rate = 1.26 l s^{-1} or 20 gpm): (a) design point; (b) gamma sensitivity; and (c) delta sensitivity.

original case study, as well as that with the lower-conductivity lens, are analyzed. The table indicates that failure to meet the target cleanup level increases significantly for the case with the lens. This emphasizes the importance of accounting for the material variability and heterogeneity when designing aquifer remediation systems. Failure to account for this factor will reduce the chances of success to meet the predetermined target cleanup standards within the specified time.

Fig. 10a, b, and c illustrates the design point, gamma, and delta sensitivities,

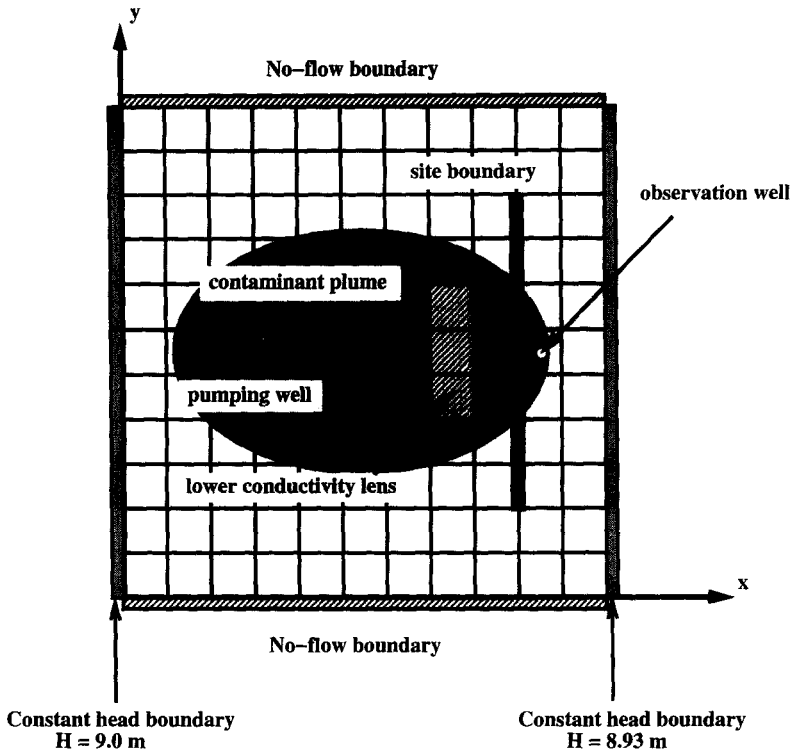


Fig. 9. Setup of the plume containment case study with a lower-conductivity lens.

respectively, for the case with the lens, and for a pumping rate of 5.68 l s^{-1} (90.0 gpm). Comparison of the trends in these figures with their counterparts for the original case (Fig. 8) indicates that when the lower-conductivity lens is present, the failure probability is most sensitive to the region downgradient from the pumping well, in addition to the region around the lens. This is another indication of the significance of careful site

Table 6
FORM failure probabilities for different pumping rates for the remediation case study

Pumping rate in l s^{-1} (gpm)	Without a lower conductivity lens		With a lower conductivity lens	
	P_F	β	P_F	β
1.89 (30.0)	0.410	0.227	0.985	-2.121
3.15 (50.0)	0.137	1.095	0.794	-0.821
4.42 (70.0)	0.061	1.556	0.526	-0.066
5.68 (90.0)	0.014	2.189	0.321	0.464

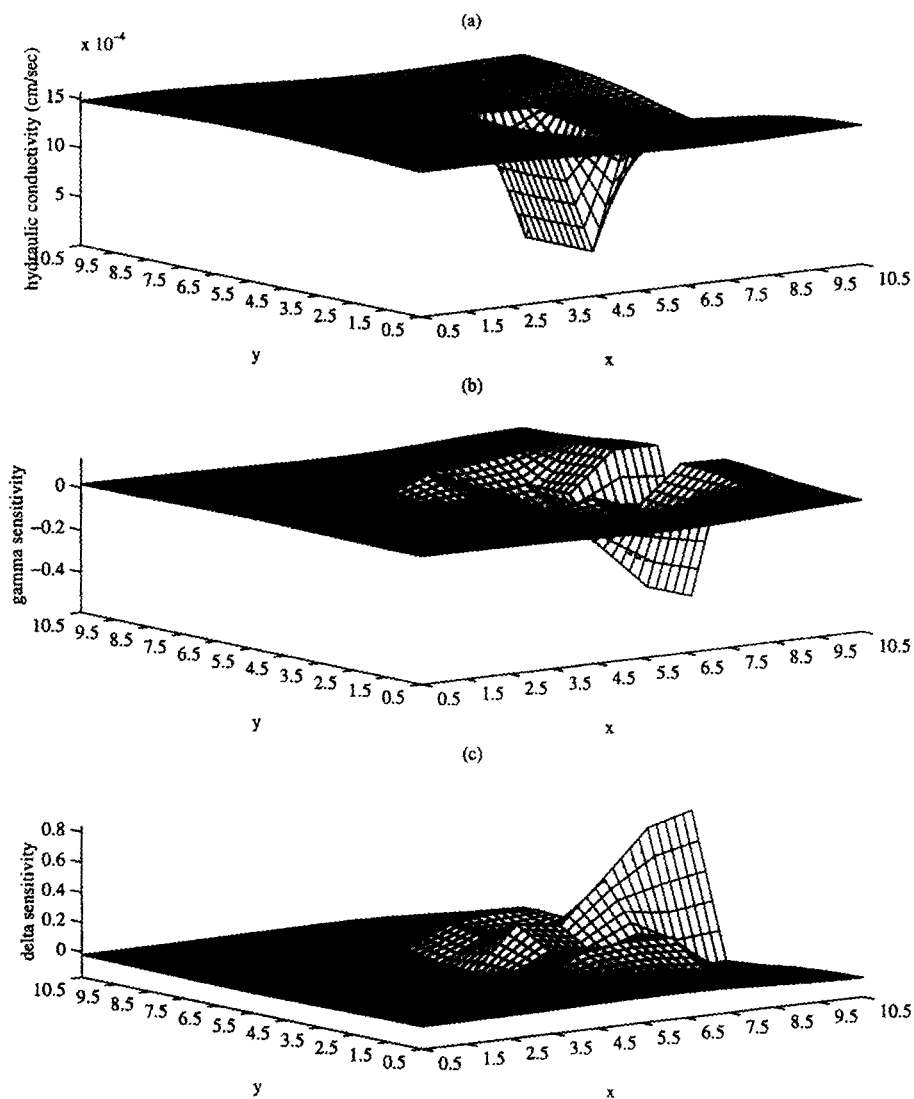


Fig. 10. Results for the plume containment with a lower-conductivity lens case study: (a) design point; (b) gamma sensitivity; and (c) delta sensitivity.

investigation to delineate the extent of heterogeneity present at the site before designing a remediation system.

5. Conclusions

The objective of this work was to present the application of the first- and second-order reliability methods (FORM and SORM) to the probabilistic modeling of groundwater

contaminant transport and plume containment. The problem was formulated in terms of probability of exceeding some target concentration value within a specified simulation time at a given point, or several points, in the aquifer. FORM and SORM provided the probability of failure, as well as sensitivity of such a probability with respect to basic uncertainty in the random variables.

The effect of spatial random variability of the aquifer was considered by modeling the hydraulic conductivity as a spatial random field with a prescribed marginal probability distribution and a correlation coefficient function. The failure probability was found to be most sensitive to the basic uncertainty in grid block conductivity along the stream tubes that bound the transport of the chemical. In this work, we used the same mesh for the solution of the finite-element model, and for the random field discretization. However, the analysis is conducted using different discretization levels elsewhere (Hamed et al., 1996).

When analyzing failure to meet the target levels at more than one location, system reliability was used. Series system formulation was used since failure to meet the predetermined target concentration at *any* well results in the failure of the system. Based on the individual (component) failure probabilities and the joint failure probabilities of any two modes, lower and upper bounds on the system failure probability were obtained.

The effect of aquifer material random heterogeneity on achieving the desired cleanup or containment goals was studied. The presence of a lower-conductivity formation was found to dramatically increase the probability of failure to meet the predetermined cleanup level within the specified operation time. This implies that accurate delineation of material heterogeneity is useful before designing aquifer remediation systems.

FORM and SORM are valuable tools for the probabilistic analysis of groundwater transport and remediation problems, especially for low-probability events. The sensitivity information provided as a by-product of a FORM reliability analysis is very useful in quantifying the value of the available data and in designing optimal data collection strategies. Nevertheless, limitations of the reliability methods should be identified. For example, FORM and SORM could become numerically intensive for large problems with many uncertain variables, where many function evaluations are needed to numerically estimate the gradients required by the optimization algorithm to determine the design point. Analytical estimation of the required gradients would alleviate this problem.

Although results presented in this work are dependent on problem setup and prescribed probability distributions, the approach is general and can be applied on any site. The findings of this work should help improve our understanding of the intricate interactions between the deterministic physical models, and the stochastic nature of porous media.

Acknowledgements

Although the research described in this article was supported by EPA through Assistance Agreement No. CR-821906 to Rice University, it has not been subjected to

Agency review and therefore does not necessarily reflect the reviews of the Agency, and no official endorsement should be inferred. Clint Dawson is gratefully acknowledged for providing the flow and transport code.

References

- Bakr, A.A., Gelhar, L.W., Gutjahr, A.L. and MacMillan, J.R., 1978. Stochastic analysis of spatial variability in subsurface flows, I. Comparison of one- and three-dimensional flows. *Water Resour. Res.*, 14(2): 263–271.
- Breitung, K., 1984. Asymptotic approximation for multinormal integrals. *J. Eng. Mech., Am. Soc. Civ. Eng.*, 110(3): 357–366.
- Cawfield, J.D. and Wu, M.-C., 1993. Probabilistic sensitivity analysis for one-dimensional reactive transport in porous media. *Water Resour. Res.*, 29(3): 661–672.
- Dawson, C.N., 1993. Gudonov-mixed methods for advection–diffusion equations in multidimensions. *SIAM J. Numer. Anal.*, 30(5): 1315–1332.
- Der Kiureghian, A. and Ke, J.-B., 1985. Finite element based reliability analysis of frame structures. *Proc. 4th Int. Conf. on Structural Safety and Reliability, Vol. I, Kobe*, pp. 395–404.
- Der Kiureghian, A. and Ke, J.-B., 1988. The stochastic finite element method in structural reliability. *Probabil. Eng. Mech.*, 3(2): 83–91.
- Der Kiureghian, A. and Liu, P.-L., 1986. Structural reliability under incomplete probability information. *J. Eng. Mech., Am. Soc. Civ. Eng.*, 112(1): 85–104.
- Der Kiureghian, A., Lin, H.-Z. and Hwang, S.-J., 1987. Second order reliability approximations. *J. Eng. Mech., Proc. Am. Soc. Civ. Eng.*, 113(8): 1208–1225.
- Ditlevsen, O., 1979. Narrow reliability bounds for structural systems. *J. Struct. Mech.*, 7(4): 453–472.
- Gureghian, A.B., Miklas, M., Sagar, B. and De Wispelare, A., 1994. Probabilistic performance analyses applied to four-member radionuclide decay chain migration through fractured geologic medium. *Spectrum '94 — Int. Top. Meet. on Nuclear and Hazardous Waste Management, Atlanta, GA*, pp. 1055–1063.
- Hamed, M.M., Conte, J.P. and Bedient, P.B., 1995. Probabilistic screening tool for groundwater contamination assessment. *J. Environ. Eng., Am. Soc. Civ. Eng.*, 121(11): 767–775.
- Hamed, M.M., Bedient, P.B. and Dawson, C.N., 1996. Probabilistic modeling of aquifer heterogeneity using reliability methods. *Adv. Water Resour.* (in press).
- Hasofer, A.M. and Lind, C.N., 1974. An exact invariant first-order reliability format. *J. Eng. Mech., Am. Soc. Civ. Eng.*, 100: 111–121.
- Jang, Y.-S., Sitar, N. and Der Kiureghian, A., 1994. Reliability approach to probabilistic modeling of contaminant transport. *Water Resour. Res.*, 30(8): 2435–2448.
- Liu, P.-L. and Der Kiureghian, A., 1986a. Multivariate distribution models with prescribed marginals and covariances. *Probabil. Eng. Mech.*, 1(2): 105–112.
- Liu, P.-L. and Der Kiureghian, A., 1986b. Optimization algorithms for structural reliability analysis. *Dep. Civ. Eng., Div. Struct. Eng. Struct. Mech., Univ. of California, Berkeley, CA, Tech. Rep. UCB/SESM-86/09*.
- Liu, P.-L., Lin, H.-Z. and Kiureghian, A.D., 1989. *CALREL User Manual*. Dep. Civ. Eng., Univ. of California, Berkeley, CA.
- Madsen, H.O., Krenk, S. and Lind, N.C., 1986. *Methods of Structural Safety*. Prentice-Hall, Englewood Cliffs, NJ.
- Melchers, R.E., 1987. *Structural Reliability, Analysis and Prediction*. Ellis Horwood Ser. Civ. Eng., Struct. Eng. Sect.
- Rackwitz, R. and Fiessler, B., 1978. Structural reliability under combined load sequences. *Comput. Struct.*, 9: 489–494.
- Schanz, R.W. and Salhotra, A., 1992. Evaluation of the Rackwitz–Fiessler uncertainty analysis method for environmental fate and transport models. *Water Resour. Res.*, 28(4): 1071–1079.
- Sitar, N., Cawfield, J.D. and Der Kiureghian, A., 1987. First order reliability approach to stochastic analysis of subsurface flow and contaminant transport. *Water Resour. Res.*, 23(5): 794–804.
- Wu, M.-C. and Cawfield, J.D., 1992. Probabilistic sensitivity and modeling of two-dimensional transport in porous media. *Stochast. Hydrol. Hydraul.*, 6: 103–121.